Ion-neutral collision frequencies for calculating ionospheric conductivity

A. Ieda[1]

[1]Institute for Space-Earth Environmental Research, Nagoya University, Nagoya, Japan.

Corresponding author: Akimasa Ieda (ieda@isee.nagoya-u.ac.jp)

Key Points:

- A set of ion–neutral collision frequency coefficients for calculating the electric conductivity is summarized.
- The coefficients and collision types are compared with previous studies.
- The nonresonant collision is essential for the O_2^+–O_2 pair because the transition temperature is high.

Abstract

Molecular oxygen collides with its first positive ion in the earth's ionosphere. The collision frequency of this particle pair is used to calculate the electric conductivity. However, for this parental pair there are two collision types, resonant and nonresonant, and the selection of the collision type has been different among previous studies in calculation of conductivity. In the present study we clarify that the nonresonant collision is essential for this pair because relevant temperatures are low. That is, the peak of the ionospheric conductivity is located at altitudes between 100 and 130 km, where the temperatures of ions and neutral particles are usually lower than 600 K, for which nonresonant collision is dominant. The collision frequency would be underestimated by 30% if the resonant collision was assumed at 110-km altitude (where the temperature is 240 K). The impact of this difference on the conductivity is estimated to be small (3%), primarily because molecular nitrogen is much more abundant than molecular oxygen. Although we have confirmed that the nonresonant collision is essential, we also include the resonant type, primarily in case of possible elevated temperature events. A set of ion–neutral collision frequency coefficients for calculating the conductivity is summarized, including other particle pairs, in the Appendices. Small corrections to the classical coefficients are made.

Plain Language Summary

The earth's ionosphere is the region at altitudes between 60 and 800 km. The ionosphere consists of plasma, i.e. ions and electrons, collocated with a neutral atmosphere. Collisions between plasma and neutral atoms and molecules, such as oxygen, create an electric current. The frequencies of these collisions need to be known to calculate the electric conductivity in the ionosphere. In this study we summarize a set of collision frequencies for calculating the electric conductivity. In particular, we clarify that the nonresonant type of collision is essential between molecular oxygen and molecular oxygen ions because the temperature is low at altitudes between 100 and 130 km, where the peak of the ionospheric current is located.

1 Introduction

The earth's ionosphere is a region of weakly ionized plasmas located above approximately 60-km altitude (e.g., Brekke, 2013). In the ionosphere the electric current perpendicular to the magnetic field is concentrated mostly in the E region at altitudes between 90 and 150 km. The electric current arises from different velocities between ions and electrons. The different velocities are caused by the collisions with neutral molecules and atoms ("neutrals" hereinafter). Electron-neutral collisions are less important because electrons are strongly bound to the magnetic field. It is ion-neutral collisions that dominate the electric current and conductivity. The dominant ions are NO^+, O_2^+, and O^+, and the dominant neutrals are N_2, O_2, and O.

There are two types of collisions between ions and neutrals: nonresonant electric-polarization collisions and resonant charge-exchange collisions (e.g., Banks & Kockarts, 1973). Nonresonant collisions are possible for all ion–neutral pairs and are caused by the polarization of a neutral particle induced by an approaching ion (Figure 1a). The resonant collisions occur between ions and their parental neutrals, such as O_2^+ and O_2, and are caused by an electron jump from the parental neutral to the ion (Figure 1b). For such parental pairs, the nonresonant collision dominates at low temperatures and the resonant collision is dominant at high temperatures.

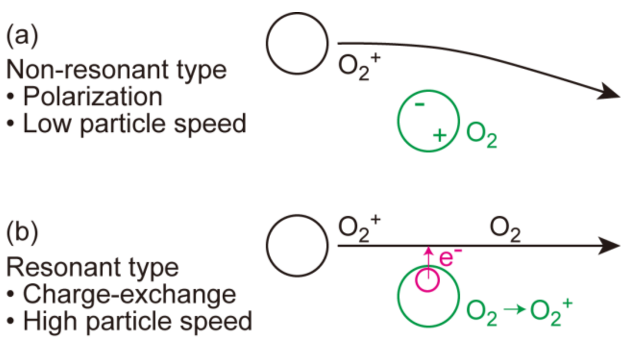

Figure 1. Two types of O_2^+–O_2 collision in the target rest frame. (a) Non-resonant type caused by the long-range polarization force. A distant collision dominant at low relative particle speeds (low temperatures). (b) Resonant type caused by electron transfer. A close collision dominant at high speeds (high temperatures).

In previous studies, it is often unclear which collision type was adopted when calculating the conductivity. The collision type adopted is sometimes not stated, or more often the study simply refers to textbooks such as Banks and Kockarts (1973) or Schunk and Nagy (2009) (hereinafter SN2009). Such previous studies implicitly assume that there is a consensus for selecting the collision type in calculations of ionospheric conductivities. However, in reality, different collision types have been used in previous studies. The resonant collision is adopted for the O_2^+–O_2 pair in some studies (e.g., McGranaghan et al., 2015; Moro et al., 2016), while some other studies adopt the nonresonant collision for this pair (e.g., Brekke & Hall, 1988; Ieda et al., 2014).

The purpose of the present study is to summarize a set of collision frequencies to calculate the ionospheric conductivity. For this, we clarify the appropriate type of O_2^+–O_2 collision to apply. We confirm that the nonresonant collision type is essential, while we conclude that the resonant type should also be included for robustness. We summarize the set of collision frequency coefficients in Appendix A. The coefficients are slightly corrected from the traditional values as calculated in Appendices B and C.

2 Temperature in the E Region

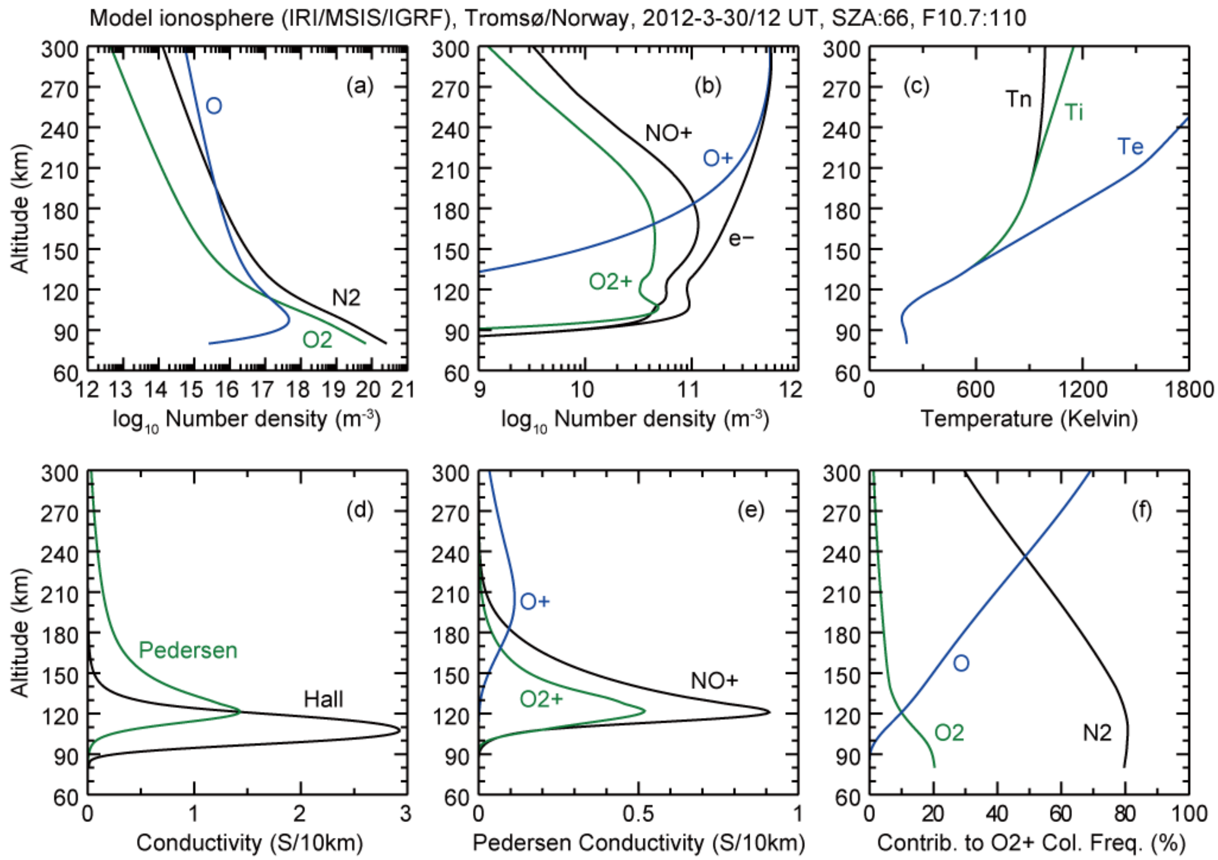

Figure 2. Altitude profiles of a model ionosphere above Tromsø, Norway (69.6°N, 19.2°E, 67° in in magnetic latitude) at 12 UT on 30 March 2012. The local noon is 1047 UT. The plasma and neutral parameters are respectively obtained from the International Reference Ionosphere (IRI) 2016 model (Bilitza et al., 2017) and the Mass Spectrometer and Incoherent Scatter (MSIS) model (Picone et al., 2002). The International Geomagnetic Reference Field (IGRF-12) model (Thebault et al., 2015) is also used to calculate conductivities. (a) Number densities of neutral atmosphere (N_2, O_2, O). (b) Number densities of ions (NO^+, O_2^+, O^+) and electrons. (c) Neutral, ion, and electron temperatures. (d) Electric conductivity (Hall and Pedersen components). (e) Ion components (NO^+, O_2^+, O^+) of the Pedersen conductivity. (f) Relative contribution of N_2, O_2, O to the O_2^+ collision frequency.

Figure 2 shows altitude profiles of a model ionospheric physical quantities above Tromsø, Norway (69.6°N, 19.2°E) at 12 UT on 30 March 2012. We selected this model example because it has a moderate solar index (F10.7 = 110) and because an interval of this day was used in our previous study (Ieda et al., 2014). Figure 2a shows the number density of major neutral species (N_2, O_2, O). Figure 2b shows the number densities of major charged species (NO^+, O_2^+, O^+, e^-). Collisions between these neutral and charged particles create the electric conductivities.

We calculate the conductivities using a method essentially the same as that of Brekke and Moen (1993) and SN2009, as follows. For a charged particle species *j* (NO^+, O_2^+, O^+, e^-), we define Ω_j

(1/s) as the gyro frequency and ν_j (1/s) as the momentum transfer collision frequency (total of the collisions with N_2, O_2, O). Using the mobility $k_j \equiv \Omega_j / \nu_j$, the conductivity for each charged species is

$$\left(\sigma_{//,j}, \sigma_{P,j}, \sigma_{H,j}\right) = \frac{en_j}{B}\left(k_j, \frac{k_j}{1+k_j^{\,2}}, \frac{k_j^{\,2}}{1+k_j^{\,2}}\right) \tag{1}$$

where //, *P*, and *H* refer respectively to the parallel, Pedersen, and Hall components. The contributions of ion species are summed so that, for example,

$$\sigma_{H,i} \equiv \sum_{j=\mathrm{NO}^+,\mathrm{O_2}^+,\mathrm{O}^+} \sigma_{H,j} \tag{2}$$

where *i* refers to the sum of ion species. The total conductivities are

$$\left(\sigma_{//}, \sigma_P, \sigma_H\right) = \left(\sigma_{//,e} + \sigma_{//,i}, \sigma_{P,e} + \sigma_{P,i}, \sigma_{H,e} - \sigma_{H,i}\right) \tag{3}$$

where *e* refers to electrons.

Figure 2c shows the neutral, ion, and electron temperatures. These temperatures are close to each other in the E region, particularly in the model data. The temperatures typically increase linearly with altitude in the E region and approach 1000–2000 K in the F region (above 150 km altitude). Figure 2d shows the Hall and Pedersen conductivities, which have peaks at altitudes between 100 and 130 km, as is typical. Note also that the O_2^+ contribution to the Pedersen conductivity (Figure 2e) has a peak at altitudes lower than the Pedersen peak altitude (Figure 2d). At these altitudes below 130 km, both the neutral and ion temperatures are lower than 600 K in Figure 2c, as is typical.

3 Collision Type Depending on Temperature

Figure 3 shows the traditional O_2^+–O_2 collision frequency coefficients (Schunk & Walker, 1973; Schunk & Nagy, 2009). Two different types of collision are shown, corresponding to

$$\nu\left(\mathrm{O_2}^+ - \mathrm{O_2}\right) = 4.08\left[\mathrm{O_2}\right] \qquad (T_r < 800\ \mathrm{K,\ nonresonant}) \tag{4}$$

$$\nu\left(\mathrm{O_2}^+ - \mathrm{O_2}\right) = 0.259\left[\mathrm{O_2}\right]\sqrt{T_r}\left(1 - 0.073\log_{10} T_r\right)^2 \qquad (T_r > 800\ \mathrm{K,\ resonant}) \tag{5}$$

where the definitions of the physical parameters are summarized in Table A1 in Appendix A. According to Banks (1966), the nonresonant (i.e., polarization) collision is effective below the transition temperature (800 K) and the resonant charge exchange collision is effective above the transition temperature.

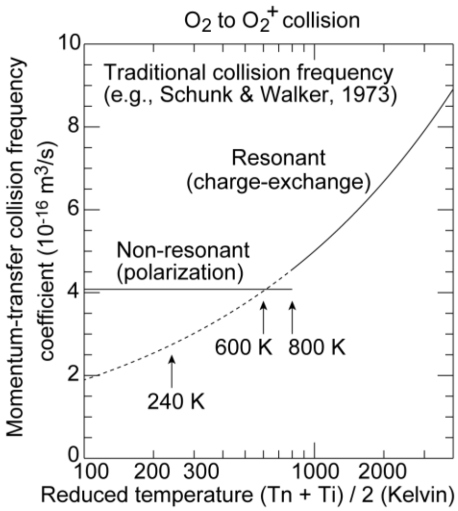

Figure 3. Traditional coefficients of the O_2^+–O_2 momentum transfer collision frequency as functions of the reduced temperature. The two lines represent the nonresonant and resonant collisions (Schunk & Walker, 1973). The nonresonant (i.e., electric-polarization) collision is effective at low temperatures, and the resonant (i.e., charge-exchange) collision is effective at high temperatures (Banks, 1966; Schunk & Walker, 1973). The transition temperature has been considered to be 800 K but appears to be approximately 600 K based on the traditional coefficients. The coefficient is 2.74 (resonant) and 4.08 (nonresonant) at 240 K.

However, the two lines in Figure 3 does not cross at 800 K but at 617 K. This is because this traditional value of 800 K for the transition temperature was likely derived in error. That is, this temperature was probably taken from Figure 3 of Banks (1966), which used an unusual value for the O_2 polarizability of 1.98, which is inconsistent with a polarizability of 1.60 in Table 1 of the same paper. We confirmed that this unusual polarizability gives a transition temperature of 808 K. The correct transition temperature should be approximately 600 K to be consistent with collision frequency coefficients listed in classic models such as Banks (1966) and Schunk and Walker (1973).

As shown in Figure 2, the neutral and ion temperatures are below approximately 600 K at the altitudes of peak conductivity. Accordingly, the nonresonant type expression in equation (4) is adequate for calculating the conductivities due to the O_2^+–O_2 collision. In particular, the relative number density of O_2^+ to other ions is highest at approximately 110 km altitude, where the temperature is 240 K in the standard atmosphere (COESA, 1976), which is much lower than 600 K. If the resonant collision was assumed at 110 km altitude, the oxygen collision frequency would be significantly (30%) underestimated.

4 Impact on the Total Conductivity

As was shown above, the resonant and nonresonant collision frequencies can be significantly different for O_2^+–O_2 pairs. We calculate the effect of this difference on the total conductivity, which also includes the contribution of other particle pairs. Figure 4a shows a 24-hour time sequence of the conductivities, electron density, and temperatures on Mar 30, 2012. The red vertical line indicates 12 UT, which corresponds to the instance of Figure 2. The electron density is the highest around the local noon at 1047 UT. The model electron, ion, and neutral temperatures do not show significant variation during a day when compared to the electron density variation.

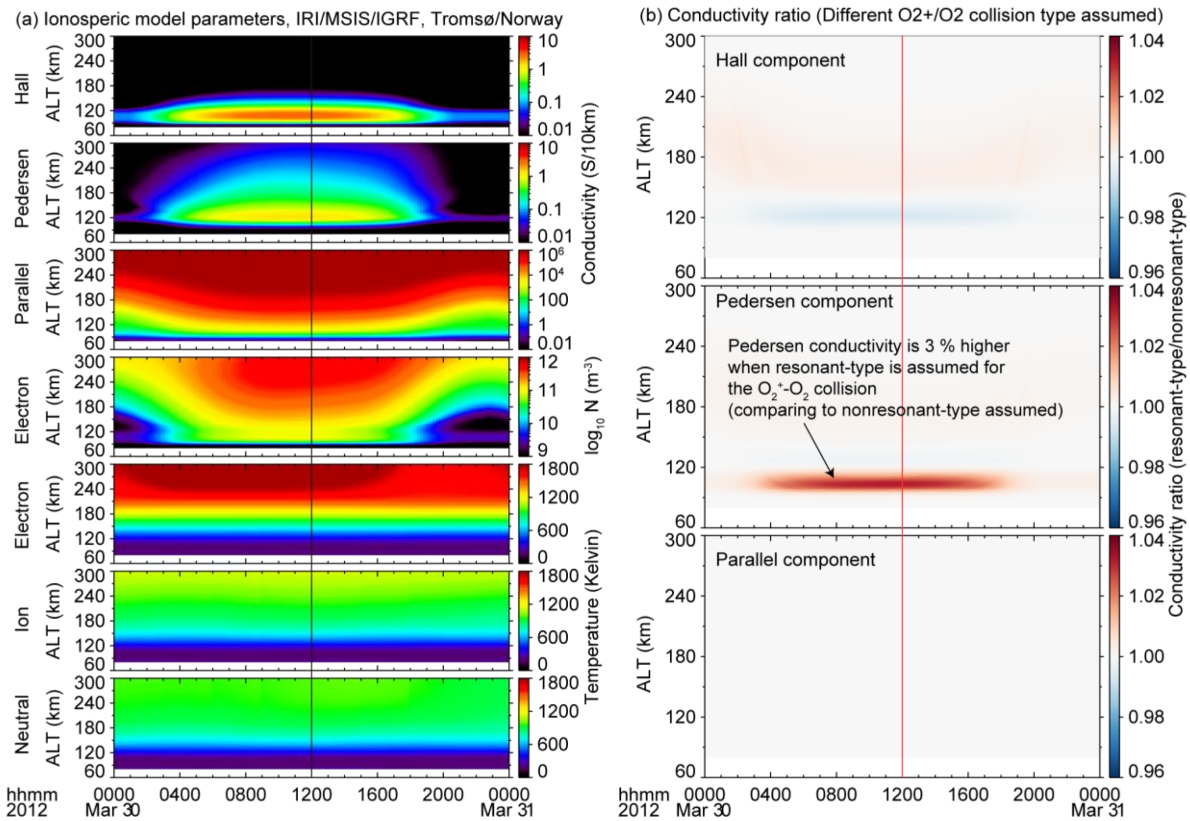

Figure 4. Time series of model ionospheric physical quantities above Tromsø, Norway (69.6°N, 19.2°E, 67° in magnetic latitude) on 30 March 2012, shown on the 10-min and 1-km grids. The vertical lines indicate 12 UT (approximately 1 hour after the local noon), corresponding to the time of Figure 2. (a) From top to bottom: calculated conductivities (Hall, Pedersen, and parallel components), model electron number density, temperatures (electron, ion, and neutral). The O_2^+–O_2 collision type depends on the temperature. (b) Ratio of the two types of conductivities, i.e., for resonant collisions and nonresonant collisions assumed for O_2^+–O_2 pairs.

We calculated two types of total conductivities assuming either the resonant or nonresonant O_2^+–O_2 collision, and then took the ratio of the two types. Figure 4b shows the ratio of the resonant type conductivity to the nonresonant type. The red color indicates that the resonant type is higher than the nonresonant type.

The overall differences between the resonant and nonresonant O_2^+–O_2 results are small (at most 3%) in Figure 4b, primarily because N_2 is typically four times more abundant than O_2 (Figures 2a and 2f) and secondly because the number density of O_2^+ is at most comparable to NO^+ (Figures 2b and 2e). Accordingly, the O_2^+–O_2 collision contributes to the total conductivity generally at most approximately 10%. Thus, the 30% underestimation of the O_2^+–O_2 collision frequency coefficient results in an impact to the total conductivity by at most approximately 3%. The maximum difference in this particular case is 3%, which would be typical during the daytime for quiet intervals.

We see that the difference is mostly in the Pedersen component in the lower E region at altitudes between 95 and 115 km during daytime. The altitude range is limited because the O_2^+ composition ratio is high only at these altitudes (Figure 2b), presumably as the result of Chapman-type solar photo-ionization. The Pedersen conductivity has a peak at 120-km altitude (Figure 2d). Below this altitude, an underestimation of the ion–neutral collision frequency corresponds to an overestimation of the Pedersen conductivity.

A weak underestimation (1%), indicated by the blue color, is seen in the Hall component near the peak Pedersen altitude (120 km), where the Hall component is sensitive to the ion–neutral collision frequency. The difference is not evident in the parallel conductivity, which is dominated by electrons.

5 Discussion

5.1 O_2^+–O_2 Collision

As detailed in the Introduction, two different types of O_2^+–O_2 collisions are considered in previous studies: the resonant type (e.g., McGranaghan et al., 2015; Moro et al., 2016) and the nonresonant type (e.g., Brekke & Hall, 1988; Ieda et al., 2014). In the present study we have clarified that the nonresonant type is usually appropriate for O_2^+–O_2 collisions for calculating the conductivity because both the neutral and ion temperatures are usually lower than approximately 600 K near the peak conductivity altitudes.

However, the ion temperature may be unusually elevated in some occasions. In addition, while the transition temperature had been traditionally recognized as 800 K, it is clarified in the present study to be 600 K. The values of 800 K and 600 K correspond respectively to altitudes of 183 km and 145 km, according to the standard atmosphere (COESA, 1976). That is, the transition altitude is no more outside the E region. Thus, it is more general to also include the resonant O_2^+–O_2 collisions.

Including both collision types is consistent with the original proposal by Banks (1966), who used either the nonresonant or resonant coefficient depending on the temperature of interest. In this regard SN2009 are not readily clear. SN2009 lists the O_2^+–O_2 collision frequency coefficient for the case above 800 K in their Table 4.5. However, SN2009 does not explicitly give the O_2^+–O_2 coefficient for the case below 800 K; thus, their table is incomplete. Confusingly, SN2009 states that the nonresonant collision occurs between unlike particles. This statement may have been interpreted that there are no nonresonant collisions for parental pairs. Note that the O_2^+–O_2 nonresonant coefficient is explicitly listed in Schunk and Walker (1973), for example.

We calculate and connect the O_2^+–O_2 resonant and nonresonant coefficients as follows. The nonresonant coefficient is calculated in Appendix B as:

$$\nu\left(\mathrm{O_2}^+ - \mathrm{O_2}\right)/\left[\mathrm{O_2}\right] = 4.08 \qquad \text{(low temperature, nonresonant)} \qquad (6)$$

See Table A1 for definitions of the parameters. We calculated the resonant coefficient in Appendix C as:

$$\nu\left(\mathrm{O_2}^+ - \mathrm{O_2}\right)/\left[\mathrm{O_2}\right] = 0.262\sqrt{T_r}\left(1-0.0735\log_{10} T_r\right)^2 \quad \text{(high temperature, resonant)} \quad (7)$$

Our calculation methods for these coefficients are essentially the same as those of the classic studies, but with small corrections.

For numerical purposes, we use the greater of equation (6) or (7) with the operator “>” as:

$$\nu\left(O_2^+ - O_2\right)/\left[O_2\right] = 4.08 > 0.262\sqrt{T_r}\left(1 - 0.0735\log_{10} T_r\right)^2 \quad (8)$$

That is, although we define the transition temperature as the temperature (607 K) at which equations (6) and (7) cross, the value is not necessary in the actual calculations of the conductivity.

We merge equations (6) and (7) in this way for simplicity. Other connection methods would be possible, for example, using spline functions. Banks (1966) emphasized that the total collision frequency is not the sum of the resonant and nonresonant frequencies. He recognized that the collision frequency is slightly enhanced (less than approximately 10%) near the transition temperature but ignored this enhancement in the final expressions.

5.2 O^+–O Collision

So far we have studied the O_2^+–O_2 collision frequency in the present study. The other parental pair relevant for the ionospheric conductivity is the O^+–O collision. For this pair the resonant collision has been traditionally selected for calculating the conductivity, presumably because this light particle pair tends to be located at high altitudes so that the relevant temperature is higher than the transition temperature (235 K in Banks and Kockarts (1973)).

This traditional value of 235 K (SN2009) appears to be an underestimate due to the 5% error in the Banks (1966) collision frequency (Appendix C). The transition temperature should be approximately 274 K. Although the nonresonant collision is probably still negligible in the earth’s recent ionosphere, we include it for robustness. Our expression is:

$$\nu\left(O^+ - O\right)/\left[O\right] = 4.01 > 0.368\cdot\sqrt{T_r}\left(1 - 0.0648\log_{10} T_r\right)^2 \quad (9)$$

where we calculate the nonresonant coefficient (i.e., 4.01) in Appendix B, and the resonant coefficients in Appendix C.

6 Conclusions

Different O_2^+–O_2 collision types have been used in previous studies. We have clarified that the nonresonant-type collision is essential because the temperature is low near the peak conductivity altitudes. Otherwise, the O_2^+–O_2 collision frequency would be significantly (30%) underestimated, though the impact of this difference on the total conductivity is estimated to be typically small (3%).

Although the nonresonant collision is essential for the O_2^+–O_2 pair, we discussed that it is more appropriate to include the resonant collision too, primarily for elevated temperature cases. In addition, the transition temperature is found to be lower (600 K) than the traditionally assumed value (800 K), which mitigates the justification for only using the nonresonant coefficients.

We summarize a set of collision frequencies for calculating the ionospheric conductivity in Appendix A. We slightly correct the collision frequency coefficients of SN2009 in Appendices A and B within the classic regime.

Appendix A: Summary of Collision Frequency Coefficients

The coefficients of the momentum transfer collision frequency are summarized in this appendix. These coefficients are used in this study to calculate the electric conductivities in the earth's ionosphere. Small corrections are made to the classic coefficient, as explained in Appendix B and Appendix C. The definitions of the physical parameters associated with the coefficients are listed in Table A1.

Table A1. *Definitions of the physical parameters associated with collision frequency*

Physical Parameters	Definition
$[\mathrm{N_2}],[\mathrm{O_2}],[\mathrm{O}]\ (1/\mathrm{m}^3)$	Number density of neutral molecular nitrogen, molecular oxygen, and atomic oxygen
ν (10^{-16}/s)	Momentum transfer collision frequency
$C\ (10^{-16}\,\mathrm{m^3/s})$	Coefficient of momentum transfer collision frequency
T_e, T_i, T_n (K)	Temperatures of electrons, ions, and neutral gases
T_r (K)	Reduced temperature, $(T_n + T_i)/2$

Note. "collision frequency" in the present study refers to the momentum-transfer collision frequency for momentum transfer from neutral particles.

Collisions of neutral (N_2, O_2, O) and charged (NO^+, O_2^+, O^+, e^-) particles are assumed to be dominant in the earth's ionosphere. There, collisions between ion and neutrals can be resonant or nonresonant. The nonresonant collision coefficients are calculated in Appendix B. The resonant collisions are calculated in Appendix C and are relevant only for parental pairs (i.e., O_2^+–O_2 and O^+–O). The parental pairs also have nonresonant coefficients. The merged coefficients of the parental pairs are concluded in the Discussion to have the forms:

$$C\left(\mathrm{O_2}^+ - \mathrm{O_2}\right) \equiv \nu\left(\mathrm{O_2}^+ - \mathrm{O_2}\right)/\left[\mathrm{O_2}\right] = 4.08 > 0.262\sqrt{T_r}\left(1 - 0.0735\log_{10} T_r\right)^2 \quad \text{(A1)}$$

$$C\left(\mathrm{O}^+ - \mathrm{O}\right) \equiv \nu\left(\mathrm{O}^+ - \mathrm{O}\right)/\left[\mathrm{O}\right] = 4.01 > 0.368\sqrt{T_r}\left(1 - 0.0648\log_{10} T_r\right)^2 \quad \text{(A2)}$$

where the operator ">" indicates the greater of the two coefficients (i.e., the nonresonant or resonant).

Using these parental-pair merged-coefficients and the unlike-pair nonresonant coefficients, the coefficients for each ion species are expressed as follows:

$$\begin{pmatrix} \nu\left(\mathrm{NO}^+\right) \\ \nu\left(\mathrm{O_2}^+\right) \\ \nu\left(\mathrm{O}^+\right) \end{pmatrix} = \begin{pmatrix} 4.36 & 4.28 & 2.45 \\ 4.15 & C\left(\mathrm{O_2}^+ - \mathrm{O_2}\right) & 2.32 \\ 6.85 & 6.66 & C\left(\mathrm{O}^+ - \mathrm{O}\right) \end{pmatrix} \begin{pmatrix} [\mathrm{N_2}] \\ [\mathrm{O_2}] \\ [\mathrm{O}] \end{pmatrix} \quad \text{(A3)}$$

The coefficients of the electron–neutral collision frequencies are adopted from SN2009 as follows:

$$\nu\left(e^-\right) = 0.233\left(1-1.21\times10^{-4}T_e\right)T_e\left[N_2\right] + 1.82\left(1+3.6\times10^{-2}\sqrt{T_e}\right)\sqrt{T_e}\left[O_2\right] + 0.89\left(1+5.7\times10^{-4}T_e\right)\sqrt{T_e}\left[O\right] \quad \text{(A4)}$$

Appendix B: Nonresonant Collision Frequency Coefficients

Nonresonant electric-polarization collisions occurs between all ion–neutral pairs. The coefficients of the momentum transfer collision frequency for this type are calculated in this appendix and small corrections are made to traditional coefficients.

We calculate the coefficients using the classic method (Banks, 1966; SN2009), which uses the nonresonant collision cross section form derived by Dalgarno et al. (1958). SN2009 calculated the nonresonant collision frequency coefficients using their equation 4.88 with neutral gas polarizabilities in their Table 4.1. However, their results do not perfectly match our results for several reasons as follows.

The ion–neutral nonresonant collision frequency (Equation 4.88 of SN2009) is

$$\nu_{in} = 2.21\pi n_n \frac{m_n}{m_i+m_n}\sqrt{\frac{\gamma_n e^2}{\mu_{in}}} \quad \text{(B1)}$$

where we believe that the following definitions are appropriate: fundamental charge $e(\mathrm{esu}) = 4.8032038\times10^{-10}$; neutral gas polarizability $\gamma_n\left(\mathrm{cm}^3\right)$; neutral number density $n_n\left(1/\mathrm{cm}^3\right)$, mass of ions and neutrals $m_i\left(\mathrm{g}\right), m_n\left(\mathrm{g}\right)$, and reduced mass $\mu_{in} = m_i m_n/\left(m_i+m_n\right)$.

We translate this equation into:

$$\nu_{in} = 25.879\times10^{-16} n_n \frac{m_n}{m_i+m_n}\sqrt{\frac{\alpha_0}{\mu_{in}}} \quad \text{(B2)}$$

where the units are changed to the number density of neutral particles $n_n\left(1/\mathrm{m}^3\right)$, neutral gas polarizability $\alpha_0\left(10^{-24}\mathrm{cm}^3\right)$, and mass in atomic units (i.e., N_2: 28, NO^+: 30, O_2^+/ O_2: 32, O^+/O: 16). This equation is equivalent to Equation 9 of Banks (1966) and Equation 9.73 of Banks and Kockarts (1973), where the center of mass coordinate system is used.

Equation (B2) indicates that the nonresonant coefficient of a particle pair depends on the neutral gas polarizability. The polarizabilities and resultant nonresonant coefficients in the present study are shown in Table B1. Also shown are those in previous studies. There are some differences between the present results, SN2009, and Schunk and Walker (1973).

The O_2-associated coefficients are slightly smaller in SN2009 (4.27, 6.64) than in Schunk and Walker (1973) (4.28, 6.66). Since the polarizabilities are the same between them, this is an inconsistency. SN2009 states that they use the O_2 polarizability (1.60) in their Table 4.1, which refers to Banks and Kockarts (1973), where the polarizability is in fact 1.59. Thus, the 1.60 in SN2009 is likely a typo and it should have been 1.59.

We adopt the set of polarizabilities that is likely actually used by SN2009. However, our results still do not match SN2009 (e.g., 4.36 and 4.34 for the NO^+– N_2 pair). We can marginally reproduce the coefficients in both SN2009 and Schunk and Walker (1973) only if the factor 25.879 in the equation (B2) was 25.79. That is, this potential misusage or equivalent causes resolves the remaining small inconsistency.

Table B1. *Coefficients of the ion-neutral nonresonant momentum transfer collision frequency*

Reference	Polarizability $\alpha_0\left(10^{-24}\mathrm{cm}^3\right)$	Coefficient of nonresonant collision frequency $C\left(10^{-16}\mathrm{m}^3/\mathrm{s}\right)$		
	N_2, O_2, O	NO^+– (N_2,O_2,O)	O_2^+– (N_2,O_2,O)	O^+– (N_2,O_2,O)
Present Study	1.76, 1.59, 0.77	4.36, 4.28, 2.45	4.15, 4.08, 2.32	6.85, 6.66, 4.01
SN2009, Tables 4.1 & 4.4	1.76, 1.60[a], 0.77	4.34, 4.27, 2.44	4.13, ---, 2.31	6.82, 6.64, ---
Schunk and Walker (1973), Appendix	1.76, 1.60, 0.77	4.34, 4.28, 2.44	4.13, 4.08, 2.31	6.82, 6.66, ---
Banks and Kockarts (1973), Table 9.10	1.76, 1.59, 0.79	---, ---, ---	---, ---, ---	---, ---, ---
Banks (1966), Tables 1 & 10	1.76, 1.60, 0.89[b]	---, ---, ---	---, 4.1, ---	---, ---, 4.3[c]

Note. The coefficients depend on the neutral gas polarizabilities. Dashes indicate that coefficients were not explicitly listed in the corresponding references.

[a]Typo. Should be 1.59. [b]Unit conversion error. Should be 0.77. [c]Erorr due to (b). Should be 4.0.

Appendix C: Resonant Collision Frequency Coefficients

The resonant charge-exchange collision occurs between ions and their parental neutrals. The O_2^+–O_2 and O^+–O pairs are relevant to the electric conductivity in the earth's ionosphere. The coefficients of the momentum transfer collision frequency for this type are calculated in this appendix and small corrections are made to traditional coefficients.

We calculate the coefficients using the classic method (Equations 25, 26, 28 of Banks (1966)), which is equivalent to Equation 4.151 of SN2009. Our resultant coefficients are slightly different from those of the classic models (Banks, 1966; Banks & Kockarts, 1973; SN2009). However, the coefficients should be essentially the same because the same formula (Dalgarno, 1958) and parameters (Table C1) were adopted for the charge-exchange cross section. To confirm this, we clarify the causes of the differences as follows.

Table C1. *Parameters of the charge exchange cross section used in classic models*

Collision Pair	O_2^+–O_2	O^+–O
Cross Section Parameter	$A_0 = 5.37, B_0 = 0.54$	$A_0 = 5.59, B_0 = 0.475$
Original Source	Amme and Utterback (1964)	Knof et al. (1964)
Source in Banks (1966)	Table 6	Table 4

The parameters in Table C1 are used in the charge-exchange cross section:

$$Q_E\left(\mathrm{cm}^2\right) = \left[\left(A_0 + 3.96B_0\right) - B_0 \log_{10} 2T_r\right]^2 \quad \text{(C1)}$$

The resonant momentum transfer collision frequency in the center-of-mass coordinate system is:

$$\nu_{COM} = f_0\sqrt{2T_r}\,2Q_E n_n \quad \text{(C2)}$$

where $f_0 \equiv \frac{4}{3}\sqrt{\frac{8k_B}{\pi m}}$ is a factor, where k_B is the Boltzmann constant (1.380649×10^{-16} erg/K), m is the ion or neutral mass (approximated as the same) in atomic units.

Accordingly, the momentum transfer collision frequency coefficient can be expressed as:

$$\begin{aligned} \nu_{COM}/n_n &= f_0\sqrt{2T_r}\,2\left[\left(A_0 + 3.96B_0\right) - B_0 \log_{10} 2T_r\right]^2 \\ &= 2f_0\sqrt{2}\sqrt{T_r}\left[\left(A_0 + \left(3.96 - \log_{10} 2\right)B_0\right) - B_0 \log_{10} T_r\right]^2 \end{aligned} \quad \text{(C3)}$$

C1 Banks style

Banks and Kockarts (1973) lists the coefficients as functions of $2T_r$ in the center-of-mass coordinate system as:

$$\nu_{COM}/n_n \equiv f_{BK}\sqrt{2T_r}\left[A_{BK} - B_{BK}\log_{10} 2T_r\right]^2 \quad \text{(C4)}$$

Comparing with equation (C3), the constants are:

$$\begin{cases} A_{BK} \equiv \sqrt{2}\left(A_0 + 3.96B_0\right) \\ B_{BK} \equiv \sqrt{2}B_0 \\ f_{BK} \equiv f_0 \end{cases} \quad \text{(C5)}$$

Using the cross-section parameter in Table C1, our results in this Banks style are:

$$\nu_{COM}\left(O_2^+ - O_2\right)/\left[O_2\right] = 3.4297\cdot10^{-3}\sqrt{2T_r}\left(10.618 - 0.76368\log_{10} 2T_r\right)^2 \quad \text{(C6)}$$

$$\nu_{COM}\left(O^+ - O\right)/\left[O\right] = 4.8503\cdot10^{-3}\sqrt{2T_r}\left(10.566 - 0.67175\log_{10} 2T_r\right)^2 \quad \text{(C7)}$$

These results are compared in Table C2 with Banks (1966) and Banks and Kockarts (1973). Our results are very close to Banks and Kockarts (1973). There are small differences between Banks (1966) and Banks and Kockarts (1973) for the O^+–O collision. Since Banks and Kockarts (1973) is much closer to our results, they presumably noticed and improved the errors in Banks (1966). That is, the O^+–O collision frequency is underestimated by approximately 5% in Banks (1966) in error.

Table C2. *Constants for resonant collision frequency coefficients in the Banks style*

Collision Pair	Parameters f_{BK}, A_{BK}, B_{BK} O_2^+–O_2	O^+–O
Present Study	0.0034, 10.6, 0.76	0.0049, 10.6, 0.67
Banks and Kockarts (1973), Table 9.13	0.0034, 10.6, 0.76	0.0048, 10.6, 0.67
Banks (1966), Table 10	0.0034, 10.6, 0.76	0.0047, 10.5, 0.67

Note. The three parameters are defined in equation (C5) and are used in equation (C4).

C2 Schunk style

SN2009 lists the coefficients as function of T_r in the laboratory or ionospheric coordinate system as:

$$\nu / n_n = f_{SN} \sqrt{T_r} \left[1 - \mathrm{B}_{SN} \log_{10} T_r\right]^2 \tag{C8}$$

Equation (C3) should be divided by two in this coordinate system. Accordingly, the constants are

$$\begin{cases} A_{SN} \equiv \mathrm{A}_0 + \left(3.96 - \log_{10} 2\right) \mathrm{B}_0 \\ B_{SN} \equiv \mathrm{B}_0 / A_{SN} \\ f_{SN} \equiv f_0 \sqrt{2} A_{SN}{}^2 \end{cases} \tag{C9}$$

Using the cross-section parameter in Table C1, our results in this Schunk style are:

$$\nu\left(\mathrm{O_2}^+ - \mathrm{O_2}\right) / \left[\mathrm{O_2}\right] = 0.26173 \sqrt{T_r} \left(1 - 0.073511 \log_{10} T_r\right)^2 \tag{C10}$$

$$\nu\left(\mathrm{O}^+ - \mathrm{O}\right) / \left[\mathrm{O}\right] \quad = 0.36834 \sqrt{T_r} \left(1 - 0.064820 \log_{10} T_r\right)^2 \tag{C11}$$

These coefficients are compared with SN2009 in Table C3. Our results slightly differ from SN2009. The SN2009 coefficients can be reproduced by starting from the Banks and Kockarts (1973) coefficients in Table C2. Thus, it is likely that SN2009 did not directly calculate the coefficients.

Table C3. *Constants for resonant collision frequency coefficients in the Schunk style*

Collision pair	Parameters f_{SN}, B_{SN} O_2^+–O_2	O^+–O
Present study	0.262, 0.074	0.368, 0.065
Schunk and Nagy (2009), Table 4.5	0.259, 0.073	0.367, 0.064

Note. The two parameters are defined in equation (C9) and are used in equation (C8).

Acknowledgments

A.I. wishes to thank M. Takeda, Y. Koyama, and Y. Ogawa for their helpful discussions on collision frequencies. The code of the International Reference Ionosphere (IRI) 2016 model was received from http://irimodel.org/. This work was supported by JSPS KAKENHI Grants 16K05568.

References

Amme, R. C., & Utterback, N. G. (1964). Effects of ion beam excitation of charge transfer cross section measurements. In M. R. C. McDowell (Ed.), *Atomic Collision Processes*. Amsterdam: North-Holland publishing.

Banks, P. (1966). Collision frequencies and energy transfer - Ions. *Planetary and Space Science, 14*(11), 1105-1122. https://doi.org/10.1016/0032-0633(66)90025-0

Banks, P. M., & Kockarts, G. (1973). *Aeronomy, Part A*. New York: Academic Press.

Bilitza, D., Altadill, D., Truhlik, V., Shubin, V., Galkin, I., Reinisch, B., & Huang, X. (2017). International Reference Ionosphere 2016: From ionospheric climate to real-time weather predictions. *Space Weather-the International Journal of Research and Applications, 15*(2), 418-429. https://doi.org/10.1002/2016sw001593

Brekke, A. (2013). *Physics of the upper polar atmosphere* (2nd ed.). Heidelberg: Springer.

Brekke, A., & Hall, C. (1988). Auroral ionospheric quiet summer time conductances. *Annales Geophysicae-Atmospheres Hydrospheres and Space Sciences, 6*(4), 361-375.

Brekke, A., & Moen, J. (1993). Observations of high-latitude ionospheric conductances. *Journal of Atmospheric and Terrestrial Physics, 55*(11-12), 1493-1512. https://doi.org/10.1016/0021-9169(93)90126-j

COESA. (1976). *U.S. standard atmosphere, 1976*. Washington, D.C: U.S. government printing office.

Dalgarno, A. (1958). The mobilities of ions in their parent gases. *Philosophical Transactions of the Royal Society of London. Series A, Mathematical and Physical Sciences, 250*(982), 426-439. https://doi.org/10.1098/rsta.1958.0003

Dalgarno, A., McDowell, M. R. C., & Williams, A. (1958). The mobilities of ions in unlike gases. *Philosophical Transactions of the Royal Society of London. Series A, Mathematical and Physical Sciences, 250*(982), 411-425. https://doi.org/10.1098/rsta.1958.0002

Ieda, A., Oyama, S., Vanhamäki, H., Fujii, R., Nakamizo, A., Amm, O., et al. (2014). Approximate forms of daytime ionospheric conductance. *Journal of Geophysical Research-Space Physics, 119*(12). https://doi.org/10.1002/2014ja020665

Knof, H., Vanderslice, J. T., & Mason, E. A. (1964). Interaction energies, charge exchange cross sections, and diffusion cross sections for N^+–N and O^+–O collisions. *Journal of Chemical Physics, 40*(12), 3548-3553. https://doi.org/10.1063/1.1725050

McGranaghan, R., Knipp, D. J., Solomon, S. C., & Fang, X. H. (2015). A fast, parameterized model of upper atmospheric ionization rates, chemistry, and conductivity. *Journal of Geophysical Research-Space Physics, 120*(6), 4936-4949. https://doi.org/10.1002/2015ja021146

Moro, J., Denardini, C. M., Resende, L. C. A., Chen, S. S., & Schuch, N. J. (2016). Influence of uncertainties of the empirical models for inferring the E-region electric fields at the dip equator. *Earth Planets and Space, 68*. https://doi.org/10.1186/s40623-016-0479-0

Picone, J. M., Hedin, A. E., Drob, D. P., & Aikin, A. C. (2002). NRLMSISE-00 empirical model of the atmosphere: Statistical comparisons and scientific issues. *Journal of Geophysical Research-Space Physics, 107*(A12). https://doi.org/10.1029/2002ja009430

Schunk, R. W., & Nagy, A. F. (2009). *Ionospheres : physics, plasma physics, and chemistry*. New York: Cambridge University Press.

Schunk, R. W., & Walker, J. C. G. (1973). Theoretical ion densities in lower ionosphere. *Planetary and Space Science, 21*(11), 1875-1896. https://doi.org/10.1016/0032-0633(73)90118-9

Thebault, E., Finlay, C. C., Beggan, C. D., Alken, P., Aubert, J., Barrois, O., et al. (2015). International Geomagnetic Reference Field: the 12th generation. *Earth Planets and Space, 67*. https://doi.org/10.1186/s40623-015-0228-9